

## DENSITY PROFILE OF A 413.5 M DEEP FRESH CORE RECOVERED AT MIZUHO STATION, EAST ANTARCTICA

Masayoshi NAKAWO<sup>1</sup> and Hideki NARITA<sup>2</sup>

<sup>1</sup>*Department of Applied Physics, Faculty of Engineering, Hokkaido University, Kita-13, Nishi-8, Kita-ku, Sapporo 060*

<sup>2</sup>*Institute of Low Temperature Science, Hokkaido University, Kita-19, Nishi-8, Kita-ku, Sapporo 060*

**Abstract:** Within a month after the core recovery, the density data were obtained from the dimensions and the weights of the core samples and by the hydrostatic method. The density data were corrected for the surface effect with considerations of the bubble concentration and the average bubble size. A method has been presented to estimate the *in situ* density value (without cracks) from the nominal density data with cracked samples based upon the data on total gas content. This method has been applied to the data of deep portion (below 135 m depth), where the core was cracked considerably. A reasonable depth profile of *in situ* density was thus estimated, which indicated that the shrinkage of trapped air bubbles was the main densification process of ice after the bubble close-off.

### 1. Introduction

Deep ice cores from ice sheets are of great interest in conjunction with the studies of the past climate as well as the ice sheet dynamics. The 24th Japanese Antarctic Research Expedition (JARE-24) has conducted, in 1983, a medium-depth drilling, and succeeded in recovering a 413.5 m deep core at Mizuho Station, East Antarctica.

Immediately after the cut-off from an ice sheet, the core samples start to relax with the sudden drop of the applied overburden pressure. The relaxation process takes place in association with various structural changes in the samples such as cracking, volume expansion, recrystallization and so on (*e.g.*, LANGWAY, 1958; Gow, 1971). The relaxation lasted more than a few years, but the initial change is the most significant (SHOJI and LANGWAY, 1983). It is important, therefore, to examine at the drilling site the characteristics of the core samples soon after the core recovery.

Throughout the Mizuho cores, stratigraphic observations and density measurements were made right after the cores were pulled out to the surface. Thin section analyses, measurements of total gas content and precise density measurements were made afterwards, yet within a month. This paper aims at providing the density data on the fresh core samples. Primary emphasis is laid on the deep portion of the core below the depth of the bubble close-off, since several investigations have already been carried out intensively on a density profile of shallow cores obtained previously at the same station (*e.g.*, MAENO, 1982).

## 2. Measurements

The density was measured by two methods. One was the direct method: the density was derived from the weight and the dimensions of core samples. This was comparatively easy to be employed, and was applied to most of the core samples obtained, although the overall error for the density values was as bad as  $\pm 20 \text{ kg m}^{-3}$  with this method. The measurements were made within an hour after the core recovery for depths above 135 m.

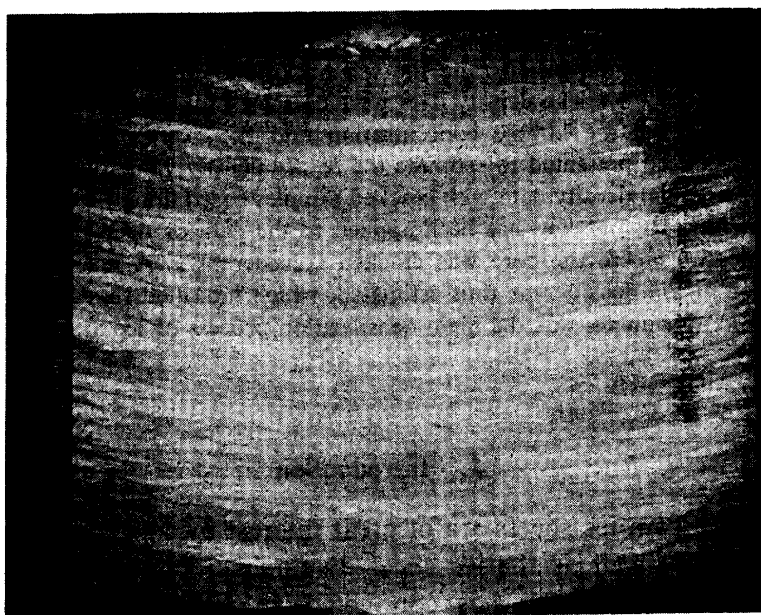


*Fig. 1. Cracked Mizuho core. 240.49–240.59 m. Cracks are convex downward.*

Below the depth of 135 m, a number of horizontal cracks were found in the cores (Fig. 1). They were probably caused by the thermal shock during drilling, since JARE-24 used a thermal drill. The cracks made the core fragile so that it was more or less difficult to handle them; the cores were stored at temperatures in a range between  $-26$  and  $-35^{\circ}\text{C}$  for one or two days, while the cracks were healed slightly. The core processing was done after the storage: the density measurements were made, for cores below 135 m, within 3 days after the core recovery.

A core of 1.0 to 1.2 m in length was obtained in each drilling; its weight, length and diameter were measured. Owing to the break off in each drilling, however, the top and bottom ends of the core were rather irregular, which would lead to a significant error in the measurements of its length. The core was hence sawed at every 0.5 m, and the weight, length and diameter measurements were made also for each 0.5 m long portion.

The horizontal cross section of the cores was not circular but rather elliptical; the diameter was measured at two principal directions orthogonal to each other. It was found that the top 0.1 m of a core obtained by each drilling was slightly smaller in diameter than the rest part of the core. This was due to the fact that the thin por-

tion of the core was drilled twice: it was drilled in the previous drilling, yet not recovered because of the level difference between the core catcher and the heater, and so it was subjected to the next drilling. The cores with the thin portion were discarded for the diameter measurements among the sawed cores of 0.5 m long. A series of horizontal steps of about 1 mm deep was found, however, continuously with intervals of a few millimeters on the vertical (side) surface of the core, corresponding to the intermittent lowering of the drill as the drilling proceeds. This irregularity at the side surface of the core caused an uncertainty in the diameter measurements.

The variation of the core diameter against depth is shown in Fig. 2. The average diameter of about 0.131 m near the surface decreased gradually with depth, reaching about 0.126 m at about 140 m in depth. At depths below 140 m, where the cores were badly cracked, the diameter was almost constant at a value of about 0.126 m, being independent of depth.

The second method adopted for the density determinations was the hydrostatic method (BUTKOVICH, 1953; LANGWAY, 1958; NAKAWO, 1980): density was determined

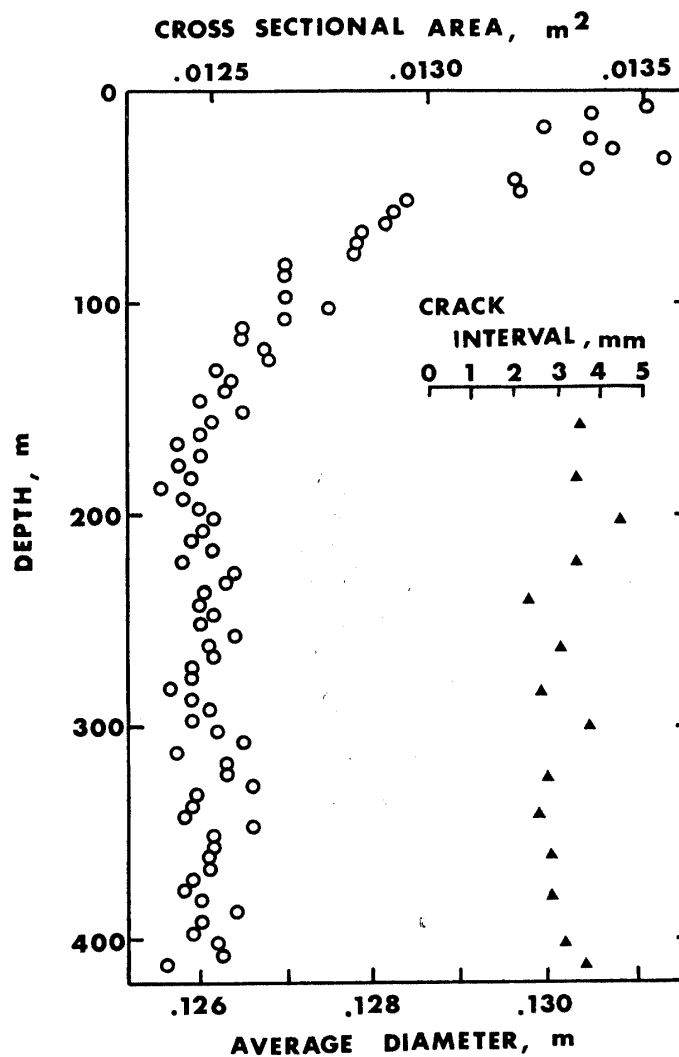


Fig. 2. Depth profiles of average diameter of the core and crack interval.

from the weight difference of a specimen in different fluids (in the air and in 2-2-4 trimethylpentane). Block samples of about 0.1 kg were cut out from the cores at every about 20 m. They were microtomed at their surfaces for the measurements. As is shown in Fig. 1, however, the samples from depths below 135 m were badly cracked, from which air could escape during weighing. These cracks were nearly horizontal, but slightly convex downward. Cautions were taken, hence, that the cracks in a specimen were placed so as to be convex upward for not releasing the air when the sample was weighed in the liquid. No air bubble release was visually observed during the measurements. The measurements were made at a temperature between  $-27$  and  $-30^{\circ}\text{C}$ . The overall accuracy of the measurements with this method was about  $\pm 0.1$  to  $0.2 \text{ kg m}^{-3}$ , depending upon the sample size.

The crack interval was measured by counting the number of cracks for a given length. The measurements were made with the density samples *per se*. The results are given also in Fig. 2. It indicates a slight decreasing trend of the crack interval with depth, but the range of the variation of the data is considerably large.

It is important to note here on the measure of the depth for the Mizuho core. The depth of a particular position of the core was determined by adding the lengths of core samples above the position in question. The depth determined by this method was slightly different from that estimated from the cable length of the drill. The details are given in Appendix, where the level is also compared with that of the cores obtained previously at the station (KUSUNOKI and SUZUKI, 1978).

### 3. Correction of the Data

#### 3.1. Surface effect

The core samples from the ice sheet contain a number of air bubbles. When a block sample was prepared from the cores, some of the bubbles were cut at the surface of the specimen. Since the liquid would fill the cut bubbles during weighing, when the hydrostatic method is adopted for the density determination, the measured volume of the sample,  $V$ , is evaluated less than the real volume by the total volume of the exposed bubbles at the surface,  $v$ . The nominal density value,  $\rho_n$ , hence becomes larger than the real one,  $\rho_t$ . They are correlated by

$$\rho_n V = \rho_t (V + v). \quad (1)$$

Since  $v$  is considered to be in proportion to the surface area of the specimen  $S$ ,

$$v = \alpha S. \quad (2)$$

The proportional constant  $\alpha$  is called the surface correction factor, which implies the total volume of the exposed bubbles at a surface of unit area.

Suppose that spherical bubbles of radius  $r$  are dispersed uniformly in an ice sample, and the concentration of bubbles is  $n$  for unit volume. With these assumption, the number of bubbles cut at the specimen surface is  $2\pi r$  per unit area, and the mean volume of an exposed bubble becomes  $2\pi r^3/3$ . Hence,

$$\alpha = \frac{4\pi r^4 \rho_t N}{3}, \quad (3)$$

where  $N$  is the bubble concentration for unit mass, given by  $n/\rho_t$ . The void ratio (total void volume per unit mass) of the specimen is given by

$$\frac{1}{\rho_t} - \frac{1}{\gamma} = \frac{4\pi r^3 N}{3}, \quad (4)$$

where  $\gamma$  is the density of pure ice. By combining eqs. (3) and (4), the surface correction factor  $\alpha$  is expressed by the following equation as a function of  $\rho_t$  for a given  $N$ .

$$\alpha = \rho_t \sqrt[3]{\frac{3}{4\pi N} \left( \frac{1}{\rho_t} - \frac{1}{\gamma} \right)^4}. \quad (5)$$

Equation (5) is shown in Fig. 3 for different values of  $N$ . At a given  $N$ ,  $\alpha$  decreased uniformly with increasing density, since the size of bubbles exposed at the surface decreases with density. For a given density a small value is obtained for  $\alpha$  with a large  $N$ , as the bubble size decreases with increasing  $N$ .

HIGASHI *et al.* (1983) obtained the values for  $\alpha$  experimentally, by measuring densities of samples with different surface area/volume ratio, using the hydrostatic method. Their samples are of ice cores obtained previously in the Mizuho Plateau, and the bubble concentration  $N$  was in a range between  $0.2 \times 10^6$  and  $0.5 \times 10^6 \text{ kg}^{-1}$  (NARITA *et al.*, 1978; ENOMOTO, unpublished). The experimental results also are plotted in Fig. 3. The data indicate larger values of  $\alpha$  than those predicted by eq. (5) for small values of density. The disagreement would be caused by the fact that the bubbles in the shallow samples, whose density is small, are not spherical but rather irregular (NARITA *et al.*, 1978), whereas bubbles were assumed spherical in eq. (5). As the density increases with depth, however, bubbles become spherical gradually and

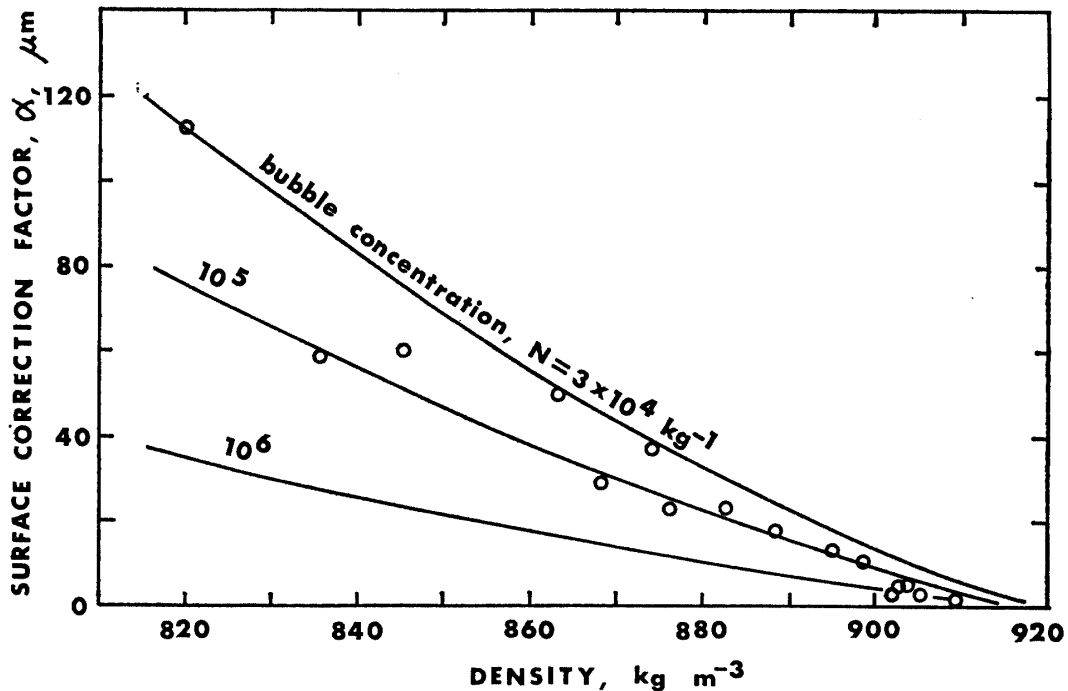


Fig. 3. Surface correction factor versus density.

the experimental data become close to the predicted curve asymptotically. The data and the prediction are in good agreement for large density values, say above  $900 \text{ kg m}^{-3}$ .

Since the bubble concentration of the 413.5 m Mizuho core was also in a range from  $0.2 \times 10^6$  to  $0.5 \times 10^6 \text{ kg}^{-1}$  (NARITA and NAKAWO, 1985), the same range as for the previous cores, the surface correction factor  $\alpha$  was estimated from the data of HIGASHI *et al.*, when their density value was smaller than  $900 \text{ kg m}^{-3}$ . For samples with larger densities, eq. (5) was used for deriving the  $\alpha$  values. With those  $\alpha$  values, the surface corrections were made for the density data of the 413.5 m Mizuho core, using eqs. (1) and (2) by the iteration method.

### 3.2. Cracks

As was mentioned before, the core samples were found cracked considerably at depths below about 135 m. Most of the cracks were observed being open at the surfaces of a block sample prepared for the density determination, although there could be internal cracks or cavities, which were isolated from the atmosphere. Some of the internal cracks could be open to an internal bubble. Also, several bubbles could be cut by open cracks, and hence become unclosed to the atmosphere. They are shown schematically in Fig. 4.

When the density of the block samples with these cracks was measured, one would underestimate its density in comparison with the value for an ideal sample with no cracks. The void ratio of the cracked samples is the sum of the volume of the bubbles,  $a_b$ , and of the open and internal cracks, denoted by  $a_f$  and  $a_i$  respectively. They are correlated with the nominal density  $\rho_n$  by the following equation,

$$\frac{1}{\rho_n} - \frac{1}{\gamma} = a_b + a_f + a_i, \quad (6)$$

where  $\gamma$  is the density of pure ice. The density for the ideal sample without cracks,

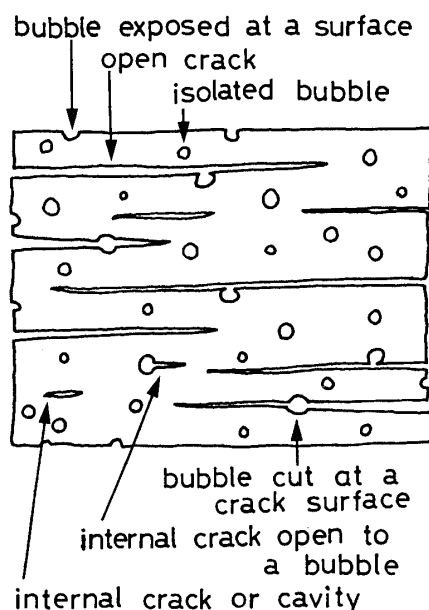


Fig. 4. Schematic figure of a cracked sample.

$\rho_m$ , on the other hand, is expressed by

$$\frac{1}{\rho_m} - \frac{1}{\gamma} = a_b. \quad (7)$$

One can estimate  $\rho_m$ , therefore, if  $a_b$  is known.

Soon after the density measurements by the hydrostatic method, the block samples were subjected to the measurements on the total gas content: they were melted in kerosine and the volume of the released air introduced into a burette was measured. The method and the various corrections were described in detail by LANGWAY (1958), and HIGASHI *et al.* (1983). The measured values were corrected for the kerosine vapor pressure and for the dissolved air in the melt water etc., but neither for the surface effect, which is similar to the surface correction for the density values described in the previous section, nor for the effects by the presence of cracks if any. The collected air was originated not only from the air bubbles but also from the cracks open at the sample surfaces. The profile of the nominal total gas content  $R_n$  for the Mizuho core is presented in Fig. 5.

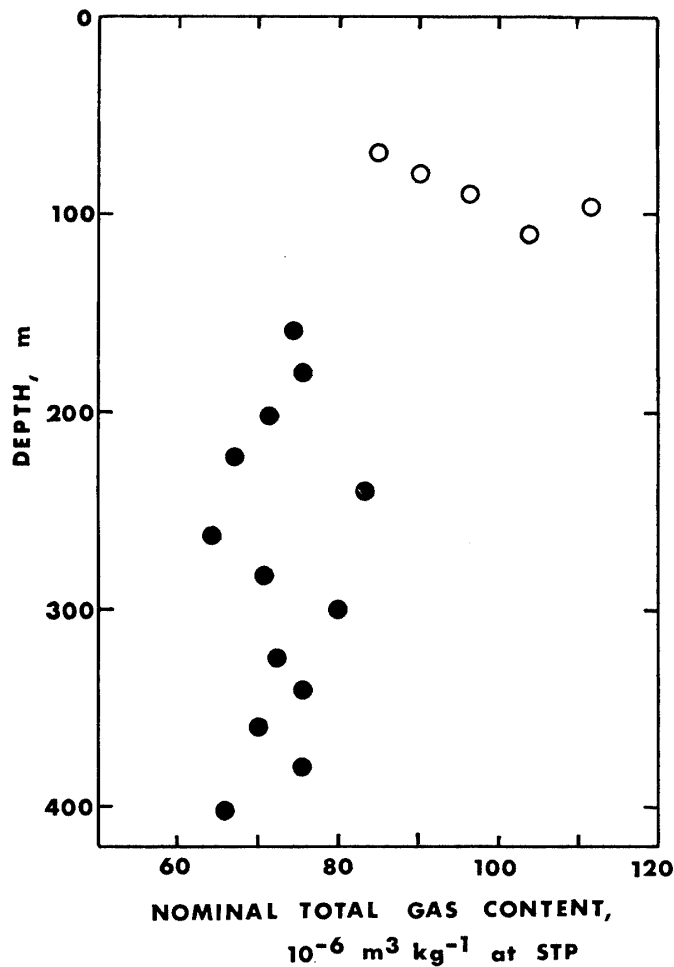


Fig. 5. Nominal total gas content against depth. Solid and open circles denote the data on samples with and without cracks respectively.

The value for  $R_n$  increased with depth, but suddenly dropped from about  $110 \times 10^{-6} \text{ m}^3 \text{ kg}^{-1}$  at a depth of 110 m to  $75 \times 10^{-6} \text{ m}^3 \text{ kg}^{-1}$  at 158 m. Below the depth, where many cracks were found in the cores,  $R_n$  fluctuated around the value of about  $70 \times 10^{-6} \text{ m}^3 \text{ kg}^{-1}$ , and are comparatively smaller than those of the shallower samples in which no cracks existed. This would indicate that some amount of the gas originally in the samples at a high pressure was released when the open cracks were formed, which could not be compensated by the gas occupying the newly formed crack space at the *in situ* atmospheric pressure. Detailed discussions on the total gas content will be given in a separate paper.

For cracked samples, the nominal total gas content  $R_n$  (described by the volume of air at STP, *i.e.* 273.15 K and 1 atm, for unit mass of the sample) is given by

$$\left(\frac{p_0}{T_0}\right) R_n = \frac{1}{T} (a_b p_b + a_t p_t + a_i p_i), \quad (8)$$

where  $T_0$  and  $T$  are the temperatures at STP and at the site respectively,  $p_0$  is the pressure at STP,  $p_b$  bubble pressure,  $p_t$  the atmospheric pressure when the samples were immersed in kerosine, and  $p_i$  the vapor pressure for ice at the *in situ* temperature. The volume of internal cracks  $a_i$  was much smaller than  $a_b$  or  $a_t$ , and  $p_i$  is definitely small in comparison with  $p_b$  or  $p_t$ . Neglecting the third term of the right side in eqs. (6) and (8), hence, the total volume of air bubbles per unit mass,  $a_b$  can be expressed by the following equation:

$$a_b = \left[ \left( \frac{T}{T_0} \right) R_n - p_t \left( \frac{1}{\rho_n} - \frac{1}{\gamma} \right) \right] / (p_b - p_t). \quad (9)$$

The values of  $a_b$  and hence  $\rho_m$  can be given by eqs. (9) and (7), therefore, if  $p_b$  is known for each sample.

The bubble pressure  $p_b$  was calculated from the data on the nominal density  $\rho_n$  and the nominal total gas content  $R_n$ . For samples with no cracks, the calculation would give the real pressure, since only the internal bubbles were taken into account for both  $\rho_n$  and  $R_n$ . For cracked samples, however, the pressure would be underestimated significantly, owing to the gas release through the formation of cracks. None the less, the calculated bubble pressure is plotted in Fig. 6, where the overburden pressure is also shown. The bubble pressure increases with depth, approaching the overburden pressure gradually. At a depth of 110 m, the difference of the two pressure values is as small as about 0.1 MPa or 1 atm. Below the depth, where the samples were all cracked, an increasing trend of  $p_b$  can also be seen, but with a large scatter. The increasing rate is much smaller than the rate of the overburden pressure, and hence the pressure difference increases with depth. The similar trends were found on ice cores obtained at various sites (LANGWAY, 1958; GOW, 1968; GOW and WILLIAMSON, 1975). Since the increase of the pressure difference with depth resulted from the cracking after the core cutting, the *in situ* bubble pressure would be very close to the overburden pressure, in particular for deep samples, as the pressure data for the non-cracked samples indicate. Assuming  $p_b$  equals to the overburden pressure, therefore, the volume of bubbles,  $a_b$  was estimated by the use of eq. (9). Accordingly,



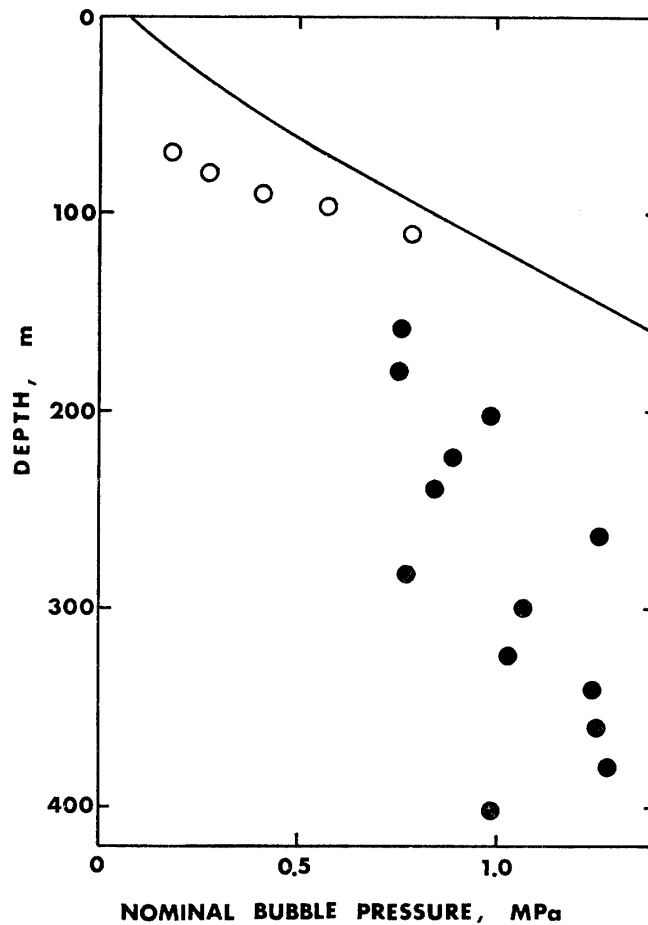


Fig. 6. Nominal bubble pressure against depth. Solid and open circles denote the data on samples with and without cracks respectively. Solid line indicates the overburden pressure.

the density  $\rho_m$ , which represents the density for ideal samples without cracks, was estimated with eq. (7).

As can be inferred by comparing eqs. (6) and (7), the ideal sample is the hypothetical one from which all the space of cracks is healed away. The volume of the crack space, however, includes the volume of many bubbles which were cut at crack surfaces (see Fig. 4). Since the nominal total gas content  $R_n$  of the cracked samples was discernibly smaller than those of non-cracked samples (Fig. 5), the volume of the cut bubbles would be very significant, and should not be neglected in the correction of the density data for the effect of cracks. For obtaining the real density value, therefore,  $\rho_m$  has to be corrected by taking into account the volume of cut bubbles at the crack surfaces. This correction is the same as the surface correction mentioned in the previous section, since the presence of many open cracks can be regarded as an increase of surface area or surface area/volume ratio. The surface area of the cracks was estimated based on the data on crack interval (Fig. 2), and the real density  $\rho_t$  was obtained by using eqs. (1) and (2), where for  $\rho_n$  one should read  $\rho_m$  and  $S$  is the area of crack surfaces.

#### 4. Density Profile

The density data obtained by the hydrostatic method is shown in Table 1 and in Fig. 7. All the data, with and without the corrections for cracks, were transformed into values at  $-35^{\circ}\text{C}$ , which is the mean ice temperature at the site (FUJII, 1978; NAKAWO, 1985a), by extrapolating the BADER's (1964) density-temperature relationship. The nominal density of the cracked samples became larger by 2 to 5  $\text{kg m}^{-3}$  through the correction for cracks. Also a large fluctuation of the data was smoothed by the correction.

Table 1. Density data by the hydrostatic method.

Depth	Nominal density at $-27.3 \pm 0.3^{\circ}\text{C}$	Remarks	Nominal total gas content	Nominal bubble pressure	Density at $-35.0^{\circ}\text{C}$ corrected for crack /surface effects
m	$\text{kg m}^{-3}$		$10^{-6} \text{ m}^3 \text{ kg}^{-1}$ (STP)	MPa	$\text{kg m}^{-3}$
69.95	886.67	no cracks	85.0	0.182	885.72
80.0	896.55	//	90.2	0.275	896.35
90.0	903.37	//	96.5	0.415	903.71
95.6	905.88	//	111.7	0.573	906.47
109.7	910.48	//	103.8	0.788	911.23
134.6	913.32	//	—	—	914.21
158.3	913.13	cracked	74.2	0.763	916.55
180.5	912.94	//	75.5	0.755	917.03
201.8	914.98	//	71.3	0.984	917.76
222.9	914.79	//	67.0	0.888	918.19
240.5	913.10	//	83.2	0.847	917.94
262.7	916.58	//	64.1	1.259	918.87
282.8	913.56	//	70.6	0.772	918.92
300.0	914.86	//	79.8	1.068	918.73
323.7	915.13	//	72.4	1.030	919.11
340.6	915.83	//	75.6	1.237	919.12
360.0	916.22	//	70.0	1.253	919.43
380.3	915.97	//	75.5	1.280	919.46
401.8	915.45	//	65.8	0.987	919.78

Avoiding the cracks, pieces of thin plate were cut out, at 5 depths, from the cracked cores. They were only a few millimeters thick and 0.01 to 0.02 kg in weight. The thin plates were subjected to the density measurements by the hydrostatic method, although the accuracy was only about  $\pm 1$  to 2  $\text{kg m}^{-3}$  because of the small sample size. The obtained density values are also plotted in Fig. 7. They are larger than the nominal values of cracked samples but smaller than the corrected at the respective depths.

No cracks were found visually in the thin piece of specimens, but there existed several fine cracks, which was revealed by a microscope. The real densities, therefore, would be larger than the measured nominal values for the thin samples. On the contrary, the real densities would be smaller than the values corrected from the data on the bulk cracked samples. This is because the surface area is greater than the values used for the corrections when the real number of existing cracks is more than that

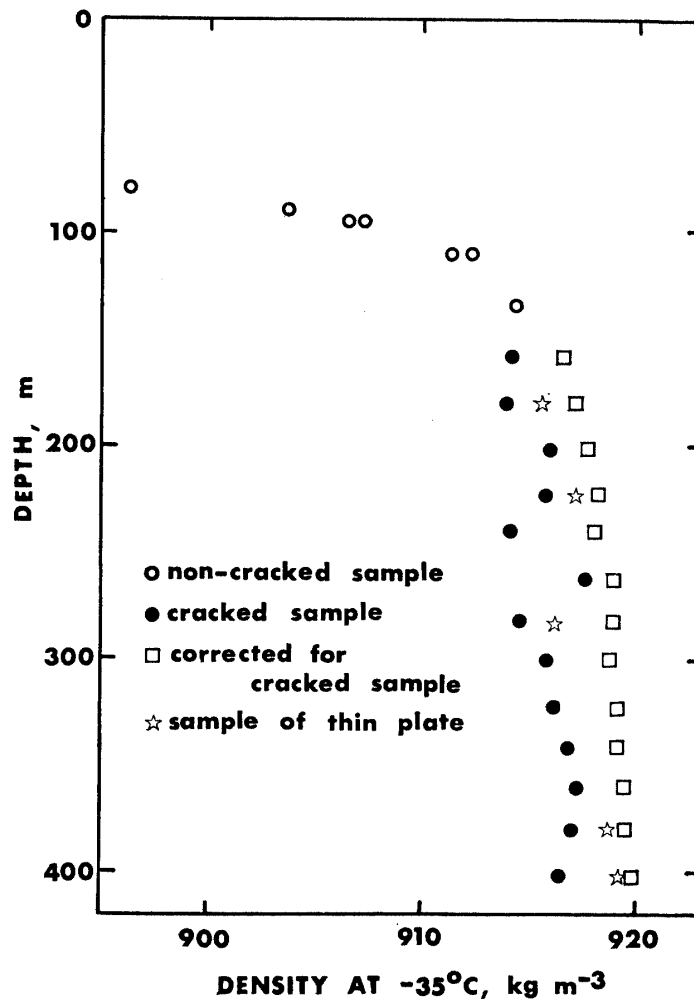


Fig. 7. Depth profile of density by the hydrostatic method.

of the visual cracks as suggested by an observation with a microscope. The corrections for the volume of bubbles cut at the crack surfaces, therefore, should be larger than the actual corrections made. The real densities, therefore, are presumably in between the values of the thin plate specimens and the corrected values from the data on cracked block samples.

Figure 8 shows all the data obtained by the direct method (the density derived from the weight and the dimensions of the core samples) as well as those by the hydrostatic method (corrected values in case of cracked samples). The data by the two methods are roughly in accordance with each other, although those by the former method are slightly smaller than those by the latter. This is because the latter data are the corrected values for cracked samples while the former are the nominal values for samples with cracks. When nominal values by the hydrostatic method are plotted, they agree very well with the data by the direct method, which, however, scatter in a wide range, corresponding to a larger error in the measurements.

Two series of density data are available on ice cores drilled previously at Mizuho Station (NARITA and MAENO, 1978). One is a measurement made at the drilling site on a 75 m long core drilled by JARE-12 in 1971, and the data are available in a range

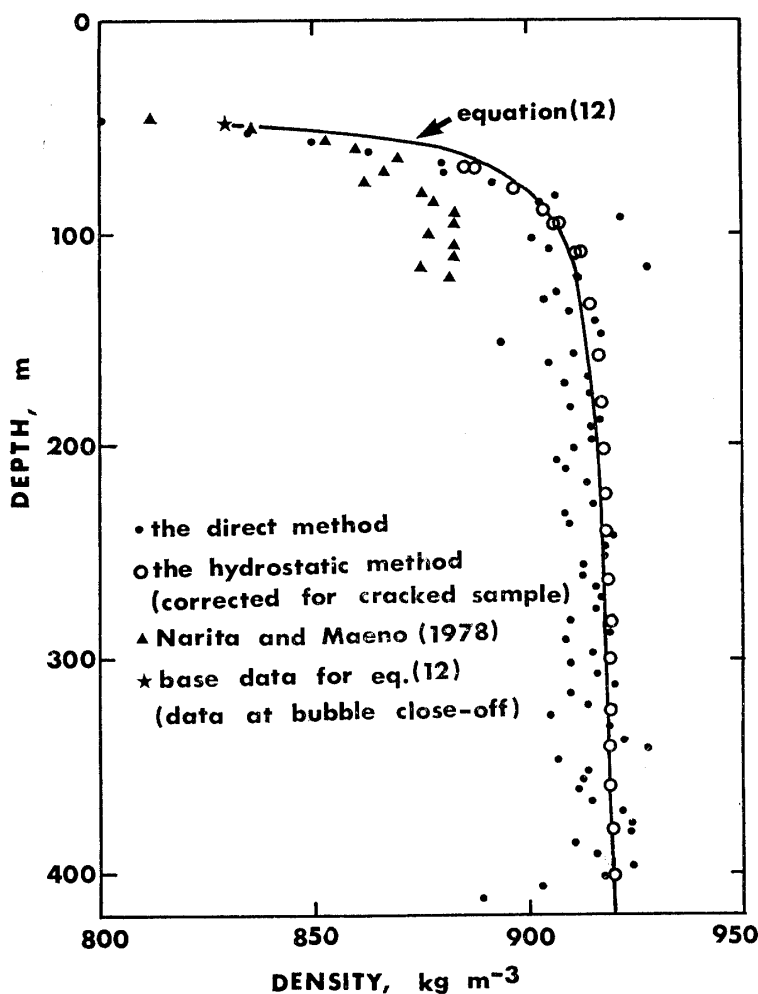


Fig. 8. Depth profiles of various densities.

of 4 to 70 m in depth. The other is the data at depths ranging from 70 to 124 m, which were obtained about one year after the core recovery on a 145 m core drilled by JARE-13 in 1972. They are also plotted in Fig. 8, where the JARE-24 data are in good agreement with the JARE-12 data (above 70 m in depth) but not with the JARE-13 data (below 70 m). The density values of the JARE-13 core is much smaller than those of the JARE-24 core. This can be explained in terms of the relaxation for about one year which the JARE-13 core was subjected to before the density measurements after the core recovery. A noticeable bending at about 70 m depth found by NARITA *et al.* (1978), on the density profile of the two series, would perhaps be attributed to the fact that the JARE-13 data (below 70 m) were those obtained after the core was relaxed. The density difference between those with one year time interval (JARE-13 core and JARE-24 core), however, is 2 to 3 kg m<sup>-3</sup> at depths between 70 and 120 m, which is considered too large to result from a simple relaxation process of contained air bubbles. Further discussion on the relaxation would be given in a separate paper.

As mentioned before, the bubble pressure at a given depth is slightly smaller but very close to the overburden pressure, which is the atmospheric pressure plus the cumulative weight of snow/ice above the depth in question. By neglecting the at-

atmospheric pressure for simplicity and for accounting the small difference between the bubble pressure and the overburden pressure,

$$p_b(z) = \int_0^z \rho g dz, \quad (10)$$

where  $p_b(z)$  is the bubble pressure at a depth  $z$ ,  $\rho$  the density at the same depth,  $g$  the acceleration of gravity. The total gas content  $R$ , on the other hand, can be given by

$$R = \left( \frac{T_0}{p_0} \right) \left( \frac{p_b}{T} \right) \left( \frac{1}{\rho} - \frac{1}{\gamma} \right), \quad (11)$$

which is similar to a combination of eqs. (6) and (8). A major difference is the absence of  $a_1$  and  $a_r$  in eq. (11), since no cracks are considered to exist under *in situ* conditions deep in the ice sheet. From eqs. (10) and (11), the following equation can be obtained by an integration with assumptions of total gas content conservation and constant temperature.

$$z - z_c = \left( \frac{p_c}{g} \right) \left( \frac{1}{\rho} - \frac{1}{\gamma} \right) \left[ \frac{\gamma(\rho - \rho_c)}{(\gamma - \rho)(\gamma - \rho_c)} - \ln \left\{ \left( \frac{\rho_c}{\rho} \right) \left( \frac{\gamma - \rho}{\gamma - \rho_c} \right) \right\} \right], \quad (12)$$

where suffix *c* indicates the values at the bubble close-off. Equation (12) represents a relationship between density  $\rho$  and depth  $z$ , which is also shown in Fig. 8. The base data for eq. (12), on the bubble close-off at Mizuho Station, were taken from HIGASHI *et al.* (1983), although the depth of the bubble close-off has some uncertainty (NAKAWO, 1985b).

The agreement between the theory and the data is fairly good, although eq. (12) predicts larger values at shallow depths, say above 100 m. This is presumably caused by an assumption, in deriving the equation, that the bubble pressure is equal to the overburden pressure, which does not hold at shallow depths (see Fig. 6). Below about 100 m, where the assumption would be applicable, the theory and the data compare very well, considering that the real density values are slightly smaller than the corrected values plotted in Fig. 8, owing to the presence of fine invisible cracks, as discussed earlier. Overall success in predicting the density profile by eq. (12) indicates that the densification would be solely attributed, after the bubble close-off, to the shrinkage of contained air bubbles, which is assumed implicitly in deriving eq. (12).

### Acknowledgments

The authors would like to thank the members of JARE-24, in particular those who shared the harsh Mizuho life, for supporting the measurements. They are also indebted to Prof. A. HIGASHI for a critical reading of the manuscript. This is a contribution from the Glaciological Research Program in East Queen Maud Land, Antarctica.

## References

- BADER, H. (1964): Density of ice as a function of temperature and stress. CRREL Spec. Rep., **64**, 6p.
- BUTKOVICH, T. R. (1953): Density of single crystals of ice from a temperate glacier. SIPRE Res. Pap., **7**, 7p.
- FUJII, Y. (1978): Temperature profile in the drilled hole. Mem. Natl Inst. Polar Res., Spec. Issue, **10**, 169.
- GOW, A. J. (1968): Bubbles and bubble pressures in Antarctic glacier ice. J. Glaciol., **7**, 167–182.
- GOW, A. J. (1971): Relaxation of ice in deep drill cores from Antarctica. J. Geophys. Res., **76**, 2533–2541.
- GOW, A. J. and WILLIAMSON, T. (1975): Gas inclusions in the Antarctic ice sheet and their glaciological significance. J. Geophys. Res., **80**, 5101–5108.
- HIGASHI, A., NAKAWO, M. and ENOMOTO, H. (1983): The bubble close-off density of ice in Antarctic ice sheets. Mem. Natl Inst. Polar Res., Spec. Issue, **29**, 135–148.
- KUSUNOKI, K. and SUZUKI, Y., ed. (1978): Ice coring project at Mizuho Station, East Antarctica, 1970–1975. Mem. Natl Inst. Polar Res., Spec. Issue, **10**, 172p.
- LANGWAY, C. C., Jr. (1958): Bubble pressures in Greenland glacier ice. Physics of the Movement of the Ice. Gentbrugge, Association Internationale d'Hydrologie Scientifique, 336–349 (IASH Publ., No. 47).
- MAENO, N. (1982): Densification rates of snow at polar glaciers. Mem. Natl Inst. Polar Res., Spec. Issue, **24**, 204–211.
- NAKAWO, M. (1980): Density of columnar-grained ice made in a laboratory. Natl. Res. Council Can., Div. Build. Res., Note, **168**, 8p.
- NAKAWO, M. (1985a): The rise of snow temperatures caused by the sewage disposal, Mizuho Station, Antarctica. Mem. Natl Inst. Polar Res., Spec. Issue, **39**, 223–232.
- NAKAWO, M. (1985b): Hyôshô-hyô no ganyû kûkiryô (Total gas content in deep ice cores). Hokkaido Daigaku Kogakubu Hôkoku (Bull. Fac. Eng., Hokkaido Univ.), **125**, 135–144.
- NARITA, H. and MAENO, N. (1978): Compiled density data from cores drilled at Mizuho Station. Mem. Natl Inst. Polar Res., Spec. Issue, **10**, 136–158.
- NARITA, H. and NAKAWO, M. (1985): Structure of 413.5-m deep ice core obtained at Mizuho Station, Antarctica. Mem. Natl Inst. Polar Res., Spec. Issue, **39**, 157–164.
- NARITA, H., MAENO, N. and NAKAWO, M. (1978): Structural characteristics of firn and ice cores drilled at Mizuho Station, East Antarctica. Mem. Natl Inst. Polar Res., Spec. Issue, **10**, 48–61.
- SHOJI, H. and LANGWAY, C. C., Jr. (1983): Volume relaxation of air inclusions in a fresh ice core. J. Phys. Chem., **87**, 4111–4114.
- SUZUKI, Y. and TAKIZAWA, T. (1978): Outline of the drilling operation at Mizuho Station. Mem. Natl Inst. Polar Res., Spec. Issue, **10**, 1–24.

*(Received May 7, 1985; Revised manuscript received September 17, 1985)*

## Appendix

*The measure of the depth for the Mizuho core*

The drilling by JARE-24 in 1983 was performed from a floor of a pit, which was at a depth of 7.67 m from the snow surface on 25 April 1983. The depth of the core was referred to this surface. A level survey revealed that the reference surface was located at 3.5 m above the 1972 snow surface, to which the depths of the JARE-12 and -13 cores, obtained in 1971 and 1972 respectively, were referred (SUZUKI and

TAKIZAWA, 1978). Namely, a given depth  $z$  of the JARE-24 core, as far as only the level is concerned, corresponds to the depth of  $z-3.53$  m for the JARE-12 and -13 cores.

The depth of a particular position of the core was derived from the cumulative length of core samples above the position in question plus 7.67 m (the depth of the pit floor from the reference surface). The depth of the bottom end of the core was thus determined to be 413.5 m.

When the bottom sample was recovered, however, the core catcher located near the bottom end of the drill was considered to be at a depth of 411.03 m, which was derived from the length of a cable suspending the drill. Another 0.07 m of core was recovered below distinguishable marks printed by the core catcher on the vertical (side) surface of the core, and hence the bottom end of the core would be at a depth of 411.10 m. The depth of the core bottom determined by this method was thus different from the depth derived from the cumulative length of the cores by more than 2 m.

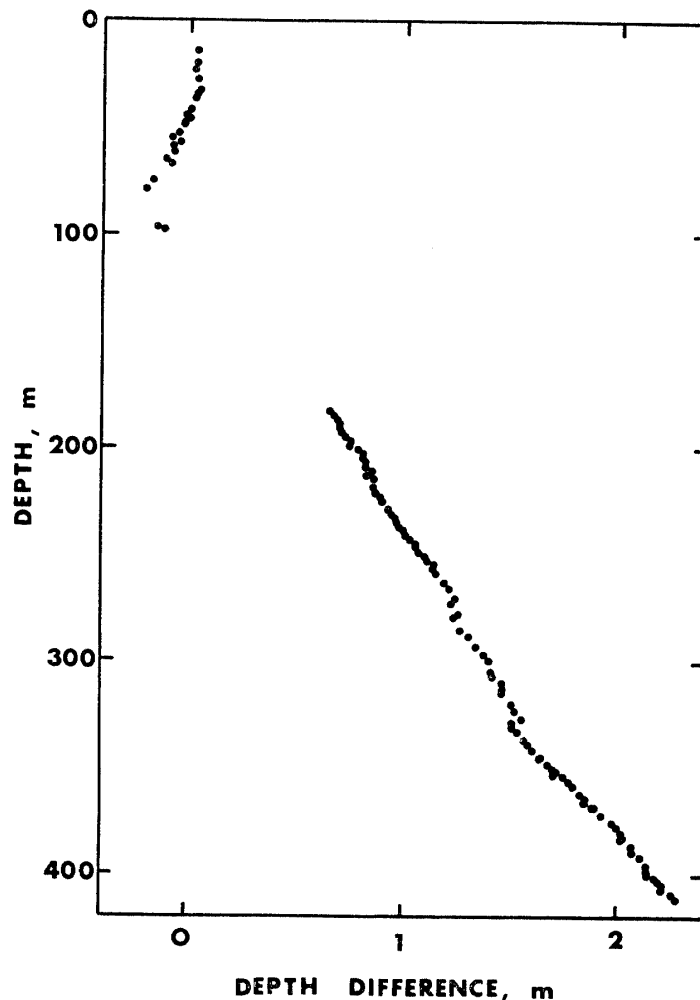


Fig. A-1. Difference between the depths estimated by the cumulative core length and by the wire length. Positive value in depth difference indicates that the former depth is larger than the latter. The comparison was not possible between the depths of 100 and 180 m, where the position of the core catcher was not marked clearly on the core surface.

At various depths also, it was possible to compare the depth level by the two methods when the marks by the core catcher were clearly recognizable on the side surface of core samples. The comparison is shown in Fig. A-1. The depths were estimated rather larger by the cumulative core lengths than by the wire length by about 0.7%, although a weak inverse trend can be seen at shallow depths above 100 m. Since the length of the cable was measured under tension, the difference would perhaps be caused by the elongation of the cores after the drilling.